Publishing Excellence Inspiring Progress
ARISTON PUBLICATIONS
Energy & Environment Advances
ISSN: xxxx-xxxx https://aristonpubs.com/energy-environment-advances https://doi.org/10.69626/eea.2024.0120

RESEARCH ARTICLE

Structural and Optical Characterizations of $ZnFe_2O_4$, $CoFe_2O_4$ and Their Nanocomposites

Nancy [1], Pradeep Kumar [2], Ritesh Verma [3,*], Preeti Thakur [1,4], Atul Thakur [4]

ABSTRACT: In this study, the structural and optical properties of zinc ferrite ($ZnFe_2O_4$), cobalt ferrite ($CoFe_2O_4$), and their nanocomposite were systematically investigated. The materials were synthesized using a co-precipitation method followed by solid-state reaction techniques. A 1:1 weight ratio was utilized for the nanocomposite to combine the distinct properties of both ferrites. Structural analysis via X-ray diffraction (XRD) confirmed the spinel cubic crystal structures for both $ZnFe_2O_4$ and $CoFe_2O_4$, with phase purity validated through Rietveld refinement. The nanocomposite demonstrated a robust crystalline structure without secondary phases. Transmission electron microscopy (TEM) revealed agglomerated crystallites within the nanometer range (10–20 nm). Optical characterization using UV-visible spectroscopy indicated semiconductor behavior with direct band gaps exceeding 2 eV, confirming their potential for optoelectronic applications. The nanocomposite exhibited enhanced structural and optical stability compared to its individual constituents, providing a promising foundation for further exploration into their magnetic and electrical properties. This study highlights the significance of $ZnFe_2O_4$, $CoFe_2O_4$, and their nanocomposite in multifunctional applications, including magnetic devices and energy storage systems.

Keywords: Spinel ferrites, Zinc ferrite, Cobalt ferrite, Nanocomposites, Optical properties

Received: 13 April 2024; Revised: 15 May 2024; Accepted: 13 June 2024; Published Online: 10 July 2024

1. INTRODUCTION

Electronics that can be powered internally without relying on external power connections are gaining immense popularity, particularly in applications demanding portability and autonomy. Integrating energy conversion and storage is pivotal for off-grid power supply, enabling more efficient management of the energy demand-supply curve—often represented as the duck curve [1]. The duck curve illustrates the discrepancy between energy availability and consumption patterns [2, 3]. Existing technologies for energy conversion and utilization generally lack efficiency due to the separation of energy storage and harvesting systems, necessitating advancements that integrate these functionalities into a single device [4].

Recent advances in nanomaterials have significantly reshaped the research landscape, particularly in terms of their ability to modify surface chemistry and optimize material properties. Nanomaterials stand apart from their bulk counterparts due to their enhanced structural, electrical, magnetic, and optical characteristics, making them a cornerstone of contemporary scientific inquiry [1]. Among the plethora of nanomaterials, magnetic nanomaterials hold a unique place, owing to their remarkable magnetic and structural properties, which find applications in diverse domains such as biomedicine, electronics, and environmental remediation [2, 3]. These properties are primarily attributed to the high surface-to-volume ratio of nanoparticles, which enhances their magnetic characteristics and other functionalities [4].

Ferrite nanoparticles have emerged as the most studied materials within the family of magnetic nanomaterials due to their wide-ranging applications, including drug delivery, gas sensing, magnetic hyperthermia, data storage, and spintronics [5, 6]. Ferrites are typically composed of iron oxides (Fe_2O_3) combined with divalent metal ions such as Zn^{2+}, Co^{2+}, or

[1] Department of Physics, Amity University Haryana, Gurugram 122413, India
[2] University Institute of Technology, Himachal Pradesh University, Shimla 171005, India
[3] Department of Physics, Graphic Era (Deemed to be) University, Dehradun 248002, Uttarakhand, India
[4] Centre for Nanotechnology, Amity University Haryana, Gurugram 122413, India

* Author to whom correspondence should be addressed: vermaritesh.rv40@gmail.com (Ritesh Verma)

Mn^{2+}. Based on structural distinctions, ferrites are categorized into three types: garnet ferrites, hexaferrites, and spinel ferrites. Spinel ferrites, represented by the general formula MFe_2O_4 (where M denotes a divalent metal ion), are particularly intriguing due to their tunable properties and suitability for numerous technological applications [7, 8].

Among spinel ferrites, zinc ferrite ($ZnFe_2O_4$) and cobalt ferrite ($CoFe_2O_4$) have garnered significant attention due to their unique properties. Zinc ferrite is known for its softness, low toxicity, and high chemical stability, making it a suitable candidate for medical applications such as drug delivery and magnetic hyperthermia [9]. On the other hand, cobalt ferrite exhibits high coercivity, moderate saturation magnetization, and excellent chemical stability, making it ideal for data storage, ferrofluids, and biosensors [10]. The magnetic and structural properties of ferrites are critically dependent on parameters such as particle size, shape, composition, and homogeneity [11]. Consequently, significant research efforts have been directed toward optimizing the synthesis and characterization of these materials to achieve the desired properties.

Several synthesis methods have been developed to produce $ZnFe_2O_4$ and $CoFe_2O_4$ nanoparticles, each offering unique advantages and challenges. Among these methods, sol-gel, hydrothermal, combustion, co-precipitation, thermal decomposition, and micro-emulsion techniques are widely employed [12]. The co-precipitation method, in particular, has emerged as a preferred choice due to its simplicity, cost-effectiveness, and ability to produce nanoparticles with high purity and uniformity [13]. This method involves the chemical precipitation of metal ions from aqueous solutions at controlled temperatures and pH conditions. The resulting nanoparticles are characterized by their small particle size, high porosity, strong chemical homogeneity, and crystallinity, making them suitable for a wide range of applications [14].

In the present study, the co-precipitation method was employed to synthesize $ZnFe_2O_4$ and $CoFe_2O_4$ nanoparticles. This approach allows for precise control over composition and structure, enabling the production of composites with tailored magnetic properties. These composites, which combine zinc ferrite and cobalt ferrite, exhibit enhanced mechanical strength, tunable magnetization, and improved electrical conductivity [15]. Such materials have potential applications in electromagnetic interference (EMI) shielding, microwave absorption, biomedical devices, and cancer treatment via magnetic hyperthermia [16].

The unique properties of zinc ferrite and cobalt ferrite composites have broadened their scope of applications across various fields. For instance, zinc ferrite's low toxicity and remarkable chemical stability make it a promising candidate for biomedical applications such as drug delivery and imaging [17]. Additionally, its softness and low saturation magnetization are advantageous for magnetic hyperthermia treatments, where controlled heating is essential for effective cancer therapy [18].

Cobalt ferrite, with its high coercivity and moderate saturation magnetization, is widely used in data storage systems, where stable magnetic properties are essential [19]. Its application in ferrofluids further enhances its utility in industrial and biomedical sectors. Furthermore, cobalt ferrite nanoparticles have been employed in spintronic devices and biosensors, leveraging their excellent chemical stability and magnetic properties [20].

The integration of zinc and cobalt ferrites into composite materials further expands their functional capabilities. These composites are particularly effective in EMI shielding, which is critical for minimizing electromagnetic interference in electronic devices. They also serve as efficient microwave absorbers, addressing the growing demand for advanced materials in telecommunications and radar systems [21]. Moreover, the combination of zinc ferrite and cobalt ferrite properties in composites enables their use in advanced biomedical applications, including drug delivery and magnetic hyperthermia [22].

The synthesis and characterization of $ZnFe_2O_4$ and $CoFe_2O_4$ nanoparticles represent a rapidly evolving field of research with significant implications for technological and biomedical advancements. The co-precipitation method, with its simplicity and efficiency, has proven to be a robust technique for producing high-quality ferrite nanoparticles. By optimizing synthesis parameters and tailoring the composition of zinc and cobalt ferrite composites, researchers can achieve materials with enhanced magnetic, electrical, and mechanical properties. These advancements pave the way for innovative applications in EMI shielding, biomedical devices, data storage, and cancer treatment.

2. EXPERIMENTAL DETAILS

2.1. Materials and Preparation of Ferrites

The ferrite nanoparticles, $ZnFe_2O_4$ and $CoFe_2O_4$, were synthesized using a chemical co-precipitation method. The raw materials employed in the synthesis included analytical-grade zinc nitrate hexahydrate ($Zn(NO_3)_2{\cdot}6H_2O$), cobalt nitrate hexahydrate ($Co(NO_3)_2{\cdot}6H_2O$), ferric nitrate nonahydrate ($Fe(NO_3)_3{\cdot}9H_2O$), and sodium hydroxide (NaOH). These chemicals were selected due to their high purity, ensuring the synthesis of ferrites with well-defined properties. To begin, a solution was prepared by dissolving the required molar ratios of the metal nitrates, i.e., zinc nitrate and ferric nitrate in distilled water. A molar ratio of 1:2 for $M(NO_3)$ and $Fe(NO_3)_3{\cdot}9H_2O$ was used to ensure the proper stoichiometric balance for the ferrite formation. This solution was then continuously stirred at a temperature of 60°C to facilitate uniform dissolution of the salts.

Simultaneously, a 1M sodium hydroxide (NaOH) solution was prepared, which was added dropwise into the metal nitrate solution to maintain a pH of approximately 7, which is critical for the precipitation of the ferrite. The dropwise addition of NaOH was controlled to avoid any rapid changes in pH, ensuring the formation of stable nanoparticles. After the addition of NaOH, the reaction mixture was allowed to age for 60 minutes at the maintained temperature and pH,

promoting the nucleation and growth of the ferrite nanoparticles.

Following this aging period, the mixture was allowed to cool to room temperature while being continuously stirred to ensure even settling of the precipitate. The precipitate was then washed several times with deionized (DI) water and acetone to remove any residual ions and impurities. The washing process involved settling the precipitate multiple times using a centrifugal separator to ensure that the ferrite particles were thoroughly cleaned.

After purification, the nanoparticles were filtered and dried in an oven at 80°C for 24 hours to remove any remaining solvent and moisture. The dried powders of zinc ferrite and cobalt ferrite were then ground into a fine powder using an agate mortar and pestle to ensure uniformity. The final step in the synthesis involved calcining the powdered ferrites in a muffle furnace at 700°C for three hours. This high-temperature treatment facilitated the formation of stable crystalline ferrite phases and improved the structural integrity of the nanoparticles.

2.2. Preparation of the Composites

For the preparation of composite ferrite materials, equal proportions (50% by weight) of zinc ferrite ($ZnFe_2O_4$) and cobalt ferrite ($CoFe_2O_4$) were selected. These ferrite weight percentages were chosen based on prior studies, which suggested that a 50:50 ratio of cobalt ferrite and zinc ferrite offers an optimal balance of properties for various applications, such as magnetic performance and structural stability. The two ferrite powders were thoroughly ground together into a fine powder using a mortar and pestle to ensure homogeneity. The resulting composite powder was stored in an airtight container until further use.

2.3. Characterizations

To characterize the structural properties of the synthesized ferrites and composites, an X-ray diffraction (XRD) analysis was conducted using a D8 Advanced X-ray diffractometer. The XRD measurements were carried out using Cu-Kα radiation (λ = 1.5406 Å), which allowed for the determination of the crystal structure, lattice parameters, and crystallite size of the ferrite nanoparticles. The data obtained from the XRD analysis also provided insights into the theoretical density of the samples. Additionally, the morphology and particle size of the nanoparticles were examined using Transmission Electron Microscopy (TEM). This technique enabled the visualization of the topographical features of the ferrite nanoparticles at high magnification, giving a detailed view of their spherical or irregular shape and size distribution. To investigate the optical properties of the synthesized materials, UV-visible spectroscopy was performed. This allowed the analysis of the absorption characteristics of the nanoparticles, providing valuable information on their potential applications in photocatalysis and other optical-related fields.

3. RESULTS AND DISCUSSION

3.1. X-ray Analysis

The structural properties of the synthesized ferrite nanoparticles were analyzed using powder X-ray diffraction (XRD). The XRD patterns, shown in Figure 1, were measured over a 2θ range from 20° to 80° to confirm the crystallinity and phase purity of the synthesized $ZnFe_2O_4$, $CoFe_2O_4$, and $CoFe_2O_4/ZnFe_2O_4$ composites. The diffraction peaks obtained from the patterns were indexed to the spinel structure, and the lattice planes identified were (220), (311), (400), (422), (511), and (440), corresponding to the typical cubic symmetry of ferrite materials. The sharp and well-defined peaks indicated the formation of highly crystalline nanoparticles, with no evidence of any secondary phases, supporting the single-phase nature of the synthesized materials.

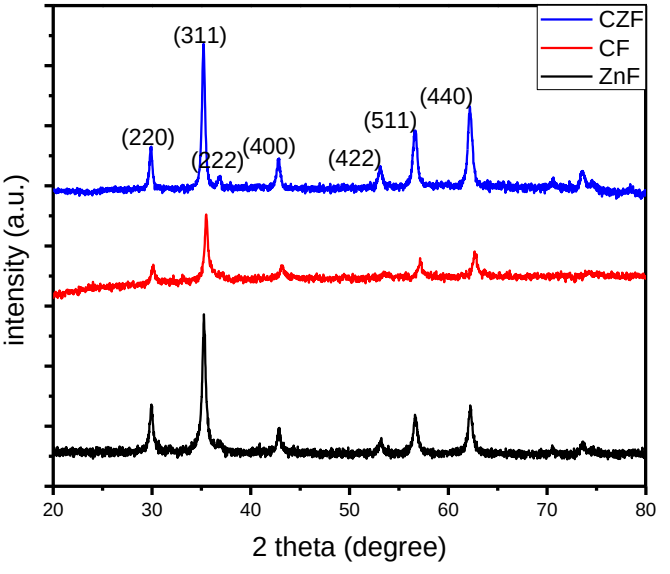

Fig. 1. The X-ray Diffraction pattern of the synthesized nanoparticles (here, ZF= Zinc ferrite, CF= Cobalt ferrite and CZF =Composite of zinc ferrite and cobalt ferrite).

The XRD data were further refined using the Fullproof program, which employs the Rietveld refinement method to extract the structural parameters of the materials. As indicated in Figure 2, the refinement confirmed that the materials exhibit a face-centered cubic (FCC) structure, which is a common crystal system for ferrites. The theoretical and experimental XRD patterns match well, with minimal deviations, as illustrated by the comparison of the red (theoretical) and black (experimental) circles.

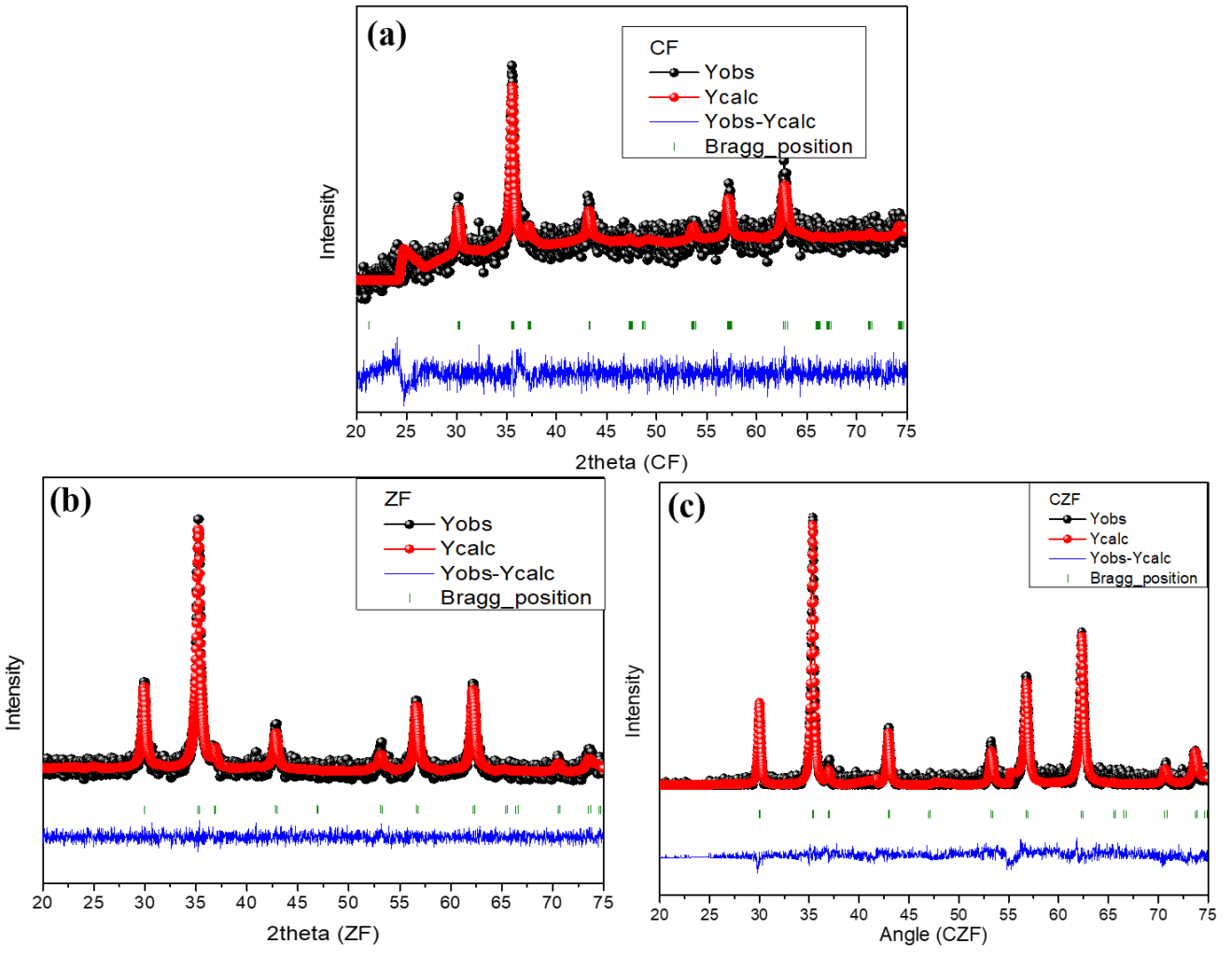

Fig. 2. Rietveld Refinement patterns of the synthesized nanoparticles.

The vertical blue lines in the figure represent the Bragg positions for the FCC structure, while the disparity between the theoretical and experimental results is shown by the blue lines.

The dislocation density and lattice strain, calculated using Williamson-Hall (W-H) plots, are provided in Figure 3 and indicate that the synthesized nanoparticles have a low dislocation density, which is indicative of high structural integrity. The low lattice strain values observed for the $CoFe_2O_4/ZnFe_2O_4$ composite suggest that the integration of zinc and cobalt ferrite does not significantly disrupt the crystal lattice, thereby preserving the stability and purity of the spinel phase.

The crystallite sizes calculated from the XRD patterns using the Scherrer equation were found to range from 10–20 nm for all the samples, as presented in Table 1. Notably, the crystallite size of cobalt ferrite ($CoFe_2O_4$) was slightly larger than that of zinc ferrite ($ZnFe_2O_4$), likely due to the larger ionic radius of Co^{2+} (0.78 nm) compared to Zn^{2+} (0.74 nm), which results in a more extensive crystal growth. This observation is consistent with previously reported studies of ferrite systems. Additionally, the lattice parameter and volume were determined, and the values for cobalt ferrite, zinc ferrite, and their composite ($CoFe_2O_4/ZnFe_2O_4$) were found to be very close to those reported in the literature, further confirming the purity and quality of the synthesized nanoparticles.

Table 1 and Table 2 provide additional structural parameters, such as lattice parameters, crystallite sizes, and bond lengths, for the synthesized ferrites. These parameters were derived from XRD data and support the consistency of the synthesized materials with the expected spinel structure. Notably, the bond lengths for $ZnFe_2O_4$ and $CoFe_2O_4$ were found to be slightly different due to the varying ionic radii of the Zn^{2+} and Co^{2+} ions, which is reflected in the different lattice constants and bond lengths. The smaller ionic radius of Zn^{2+} compared to Co^{2+} leads to a smaller lattice constant for zinc ferrite, while the larger ionic radius of Co^{2+} results in a slightly larger lattice parameter for cobalt ferrite. The composite sample, $CoFe_2O_4/ZnFe_2O_4$, exhibited intermediate values for these parameters, further indicating successful blending of the two ferrite phases.

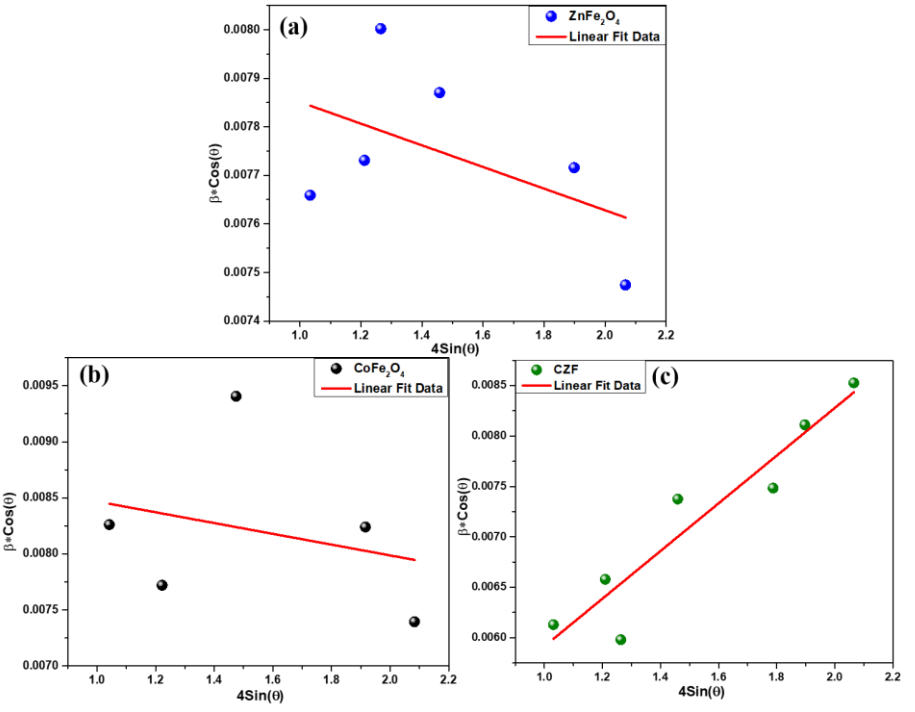

Fig. 3. The Williamson-Hall plots for synthesized nanoparticles.

Table 1. XRD parameters calculated by XRD pattern.

Parameters	Symbols	Composition		
		ZF	CF	CZF
Lattice parameter	a(Å)	8.434	8.378	8.445
Lattice volume	V(Å) ^{3}	600.010	588.136	602.472
	$d_{Scherrer}$(nm)	15.646	16.774	20.052
Crystallite size	d_{W-H} (nm)	17.181	16.774	20.052
Lattice strain	∈	-0.0002	-0.0004	0.0023
	$\delta_{Scherrer}(nm^{-2})$	0.004	0.003	0.002
Dislocation density	$\delta_{WH}(nm^{-2})$	0.003	0.004	0.0006
X-ray density	$\rho_x(g/cm^3)$	5.337	5.299	5.244

Table 2. This edge length and bond length of the prepared ferrites.

S. No.	Parameters (Å)	ZF	CF	CZF
1.	$\mathbf{d_{AX}}$	5.565	5.528	5.573
2.	$\mathbf{d_{BX}}$	2.054	2.040	2.057
3.	$\mathbf{d_{AXE}}$	3.124	3.103	3.128
4.	$\mathbf{d_{BXE}}$	2.838	2.819	2.842
5.	$\mathbf{d_{BXEU}}$	1.055	1.048	1.056
6.	$\mathbf{r_A}$	0.593	0.580	0.596
7.	$\mathbf{r_B}$	0.737	0.724	0.740
8.	**b**	2.981	2.961	2.985
9.	**c**	3.496	3.473	3.501
10.	**d**	3.647	3.623	3.652
11.	**e**	5.471	5.435	5.479
12.	**f**	5.165	5.130	5.172
13.	**p**	1.003	0.997	1.005
14.	**q**	3.739	3.714	3.744
15.	**r**	7.161	7.113	7.170
16.	**s**	6.340	6.298	6.349

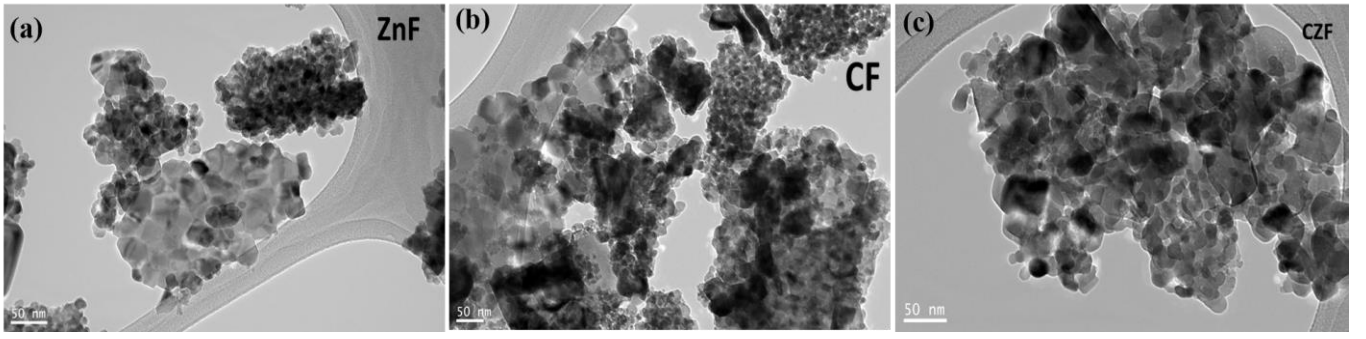

Fig. 4. TEM images of (a) Zinc ferrite, (b) Cobalt ferrite, and (c) $CoFe_2O_4/ZnFe_2O_4$.

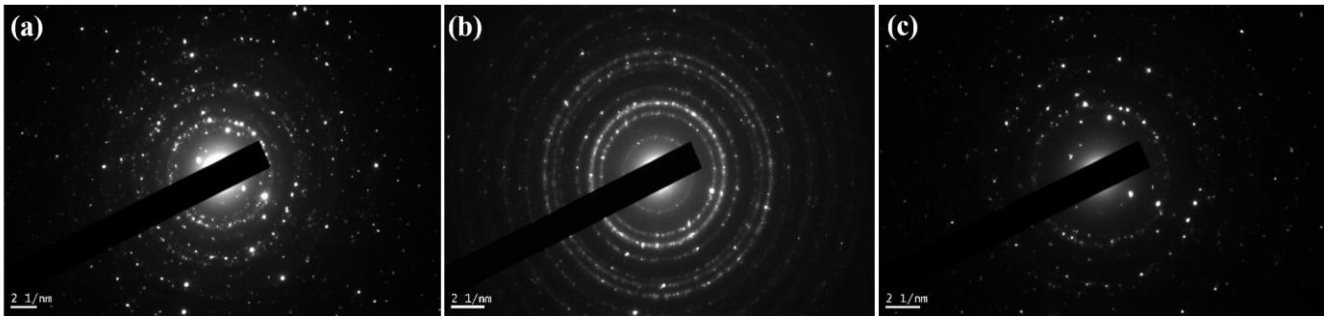

Fig. 5. SAED pattern of (a) $CoFe_2O_4$, (b) $ZnFe_2O_4$, and (c) $CoFe_2O_4/ZnFe_2O_4$.

3.2. Morphological Analysis

To further investigate the morphology and size distribution of the synthesized nanoparticles, transmission electron microscopy (TEM) and high-resolution transmission electron microscopy (HRTEM) were employed. The TEM images in Figure 4 reveal that the $ZnFe_2O_4$, $CoFe_2O_4$, and $CoFe_2O_4/ZnFe_2O_4$ samples have uniform and nanoscale sizes. The nanocrystalline nature of the materials is consistent with the XRD results. In particular, the TEM micrographs show well-dispersed nanoparticles with a size range of approximately 15–20 nm, which corroborates the crystallite sizes obtained from XRD analysis. The high-resolution TEM (HR-TEM) images further confirm the crystal structure and show clear lattice fringes, characteristic of the spinel structure. The sequential area electron diffraction (SAED) patterns, displayed in Figure 5, provide additional confirmation of the crystalline nature of the nanoparticles. The observed diffraction rings in the SAED pattern were indexed to the (220), (311), (400), and (440) planes, matching well with the XRD and HR-TEM data. The consistent SAED patterns across the three samples ($ZnFe_2O_4$, $CoFe_2O_4$, and $CoFe_2O_4/ZnFe_2O_4$) indicate the formation of a pure spinel phase without any impurity phases, confirming the successful synthesis of these nanoparticles.

3.3. UV-Vis Analysis

The optical properties of the synthesized nanoparticles were studied using UV-visible spectroscopy. Figure 6 displays the UV-visible spectra of $CoFe_2O_4$, $ZnFe_2O_4$, and $CoFe_2O_4/ZnFe_2O_4$. The spectra reveal that the cobalt ferrite nanoparticles exhibit a broad absorption in the visible region, suggesting that these nanoparticles are capable of absorbing light over a wide wavelength range. This is indicative of the potential application of $CoFe_2O_4$ in various optoelectronic and photocatalytic applications. In contrast, zinc ferrite shows no absorption tail in the UV region, and the composite ($CoFe_2O_4/ZnFe_2O_4$) also exhibits similar absorption characteristics. The optical band gap of the nanoparticles was determined by plotting $(\alpha h\nu)^2$ vs. $h\nu$ (Tauc plot), as shown in **Figure 7**. The Tauc plot was used to calculate the energy band gap (Eg) for each material using the relation:

$$\alpha h\nu = A(h\nu - E_g)^n \quad (1)$$

Where α is the absorption coefficient, $h\nu$ is the photon energy, and n is a constant that depends on the nature of the electronic transition (n = 2 for indirect transitions). The band gap values for the samples were determined as follows: $CoFe_2O_4$ (4.978 eV), $ZnFe_2O_4$ (2.693 eV), and the $CoFe_2O_4/ZnFe_2O_4$ composite (2.529 eV). The large band gap of $CoFe_2O_4$ indicates that it is a good candidate for applications requiring high resistance to light absorption in the UV region, while the smaller band gap of $ZnFe_2O_4$ and the composite suggests better optical activity in the visible region, making these materials more suitable for photocatalytic and photochemical applications.

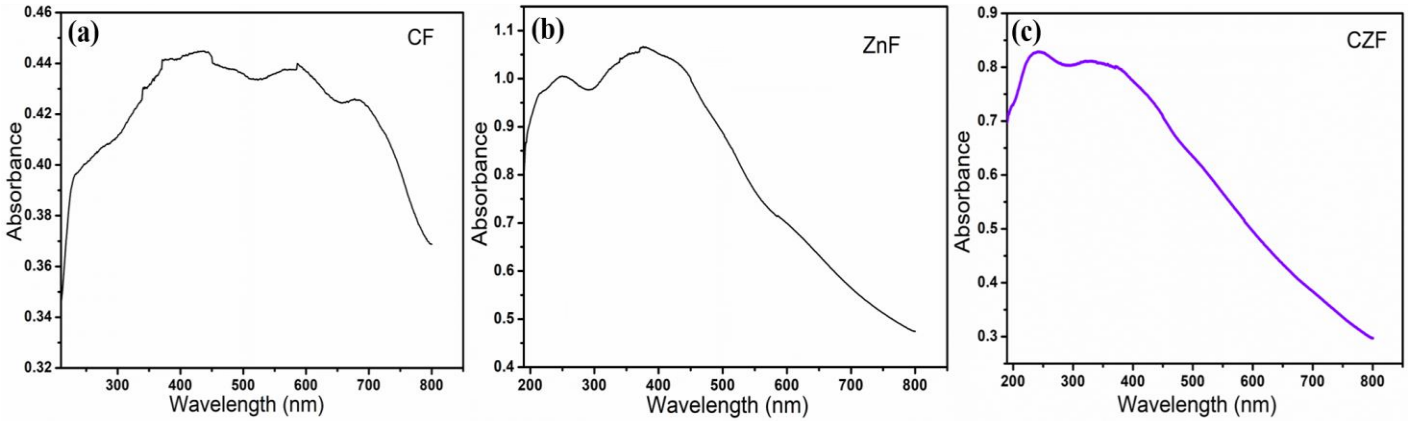

Fig. 6. UV-visible spectrum of a) Cobalt ferrite, b) Zinc ferrite, c) $CoFe_2O_4/ZnFe_2O_4$.

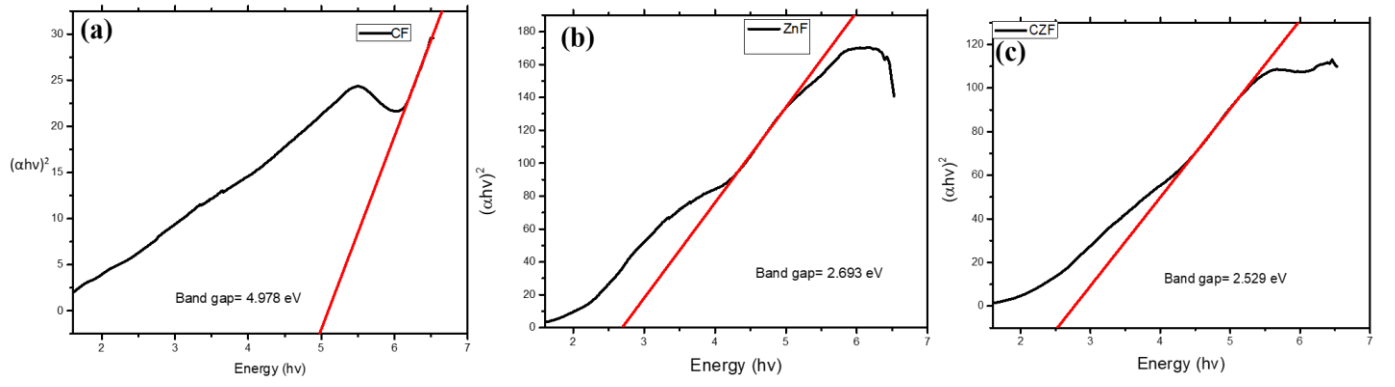

Fig. 7. Tauc plot of (a) $CoFe_2O_4/ZnFe_2O_4$ having band gap = 2.529 eV, (b) Cobalt ferrite having band gap = 4.978 eV, and (c) Zinc ferrite having band gap=2.693eV.

The XRD, TEM, UV-Vis, and other characterization techniques collectively confirm the successful synthesis of pure, single-phase zinc ferrite, cobalt ferrite, and their composite. The crystalline nature, small particle size, and favorable optical properties make these materials promising candidates for various technological applications, including photocatalysis, magnetism, and energy storage. The $CoFe_2O_4/ZnFe_2O_4$ composite exhibited superior optical and structural properties compared to individual ferrites, suggesting enhanced performance for practical applications.

4. CONCLUSION

The current investigation demonstrates the successful synthesis and characterization of zinc ferrite ($ZnFe_2O_4$), cobalt ferrite ($CoFe_2O_4$), and their nanocomposite using a co-precipitation method followed by solid-state reactions. Structural analysis confirmed that both $ZnFe_2O_4$ and $CoFe_2O_4$ exhibit pure spinel cubic phases with no impurity phases, as validated by XRD and Rietveld refinement. TEM analysis corroborated the nanocrystalline nature of these materials, with particle sizes ranging between 10–20 nm. The combination of $ZnFe_2O_4$ and $CoFe_2O_4$ in a 1:1 ratio resulted in a composite material with superior structural stability. Optical studies through UV-visible spectroscopy revealed that both the ferrites and the nanocomposite possess semiconductor characteristics with direct band gaps greater than 2 eV. The nanocomposite showed improved optical stability, demonstrating its potential for applications in optoelectronics, energy storage, and magnetic devices. These findings suggest that the nanocomposite approach could be a promising pathway for tailoring the properties of spinel ferrites for advanced technological applications. Future work will focus on investigating the magnetic and electrical properties of these materials, aiming to expand their applicability in areas such as electromagnetic shielding, spintronics, and biomedical devices. The synthesis method used in this study offers a cost-effective and scalable approach, making it suitable for industrial and commercial adoption. This work lays the groundwork for further exploration into the multifunctional potential of $ZnFe_2O_4$, $CoFe_2O_4$, and their composites.

DECLARATIONS

Ethical Approval

We affirm that this manuscript is an original work, has not been previously published, and is not currently under consideration for publication in any other journal or conference proceedings. All authors have reviewed and approved the manuscript, and the order of authorship has been mutually agreed upon.

Funding

Not applicable

Availability of data and material

All of the data obtained or analyzed during this study is included in the report that was submitted.

Conflicts of Interest

The authors declare that they have no financial or personal interests that could have influenced the research and findings presented in this paper. The authors alone are responsible for the content and writing of this article.

Authors' contributions

All authors contributed equally in the preparation of this manuscript.

REFERENCES

[1] Armaroli, N. and Balzani, V., 2007. The future of energy supply: challenges and opportunities. *Angewandte Chemie International Edition*, *46*(1-2), pp.52-66.

[2] Rao, P.A., Rao, K.S., Raju, T.P., Kapusetti, G., Choppadandi, M., Varma, M.C. and Rao, K.H., 2019. A systematic study of cobalt-zinc ferrite nanoparticles for self-regulated magnetic hyperthermia. *Journal of Alloys and Compounds*, *794*, pp.60-67.

[3] Jadhav, S.A., Somvanshi, S.B., Khedkar, M.V., Patade, S.R. and Jadhav, K.M., 2020. Magneto-structural and photocatalytic behavior of mixed Ni–Zn nano-spinel ferrites: visible light-enabled active photodegradation of rhodamine B. *Journal of Materials Science: Materials in Electronics*, *31*, pp.11352-11365.

[4] Patade, S.R., Andhare, D.D., Somvanshi, S.B., Kharat, P.B., More, S.D. and Jadhav, K.M., 2020. Preparation and characterisations of magnetic nanofluid of zinc ferrite for hyperthermia. *Nanomaterials and Energy*, *9*(1), pp.8-13.

[5] Vinuthna, C., Raju, R.M. and Ravinder, D., 2014. Preparation and Characterization of Zinc Substituted Cobalt Ferrite Nano-Particles by Citrate Gel Method. *Advances in Materials Science for Environmental and Energy Technologies III*, *250*, pp.287-297.

[6] Ding, J., Tsuzuki, T., McCormick, P.G. and Street, R., 1996. Ultrafine Co and Ni particles prepared by mechanochemical processing. *Journal of Physics D: Applied Physics*, *29*(9), p.2365.

[7] Ambrose, T., Gavrin, A. and Chien, C.L., 1992. Formation and magnetic properties of nanocomposite Fe-Al_2O_3 using high-energy ball milling. *Journal of magnetism and magnetic materials*, *116*(3), pp.L311-L314.

[8] Jogi, J.K., Singhal, S.K., Jangir, R., Dwivedi, A., Tanna, A.R., Singh, R., Gupta, M. and Sagdeo, P.R., 2022. Investigation of the structural and optical properties of zinc ferrite nanoparticles synthesized via a green route. *Journal of Electronic Materials*, *51*(10), pp.5482-5491.

[9] Sonia, L.C., Victory, M. and Phanjoubam, S., 2020. A comparative study of the properties of zinc ferrite nanoparticles synthesized by different techniques for nanofluid preparation. *Integrated Ferroelectrics*, *204*(1), pp.100-111.

[10] Nasir, S., Asghar, G., Malik, M.A. and Anis-ur-Rehman, M., 2011. Structural, dielectric and electrical properties of zinc doped nickel nanoferrites prepared by simplified sol–gel method. *Journal of Sol-Gel Science and Technology*, *59*, pp.111-116.

[11] Vinosha, P.A., Mely, L.A., Jeronsia, J.E., Monica, F.H., Raja, K. and Das, S.J., 2017. Study of Structural, optical, dielectric and magnetic properties of zinc ferrite synthesized by co-precipitation. *Nano Hybrids and Composites*, *17*, pp.1-9.

[12] Arulmurugan, R., Vaidyanathan, G., Sendhilnathan, S. and Jeyadevan, B., 2005. Co–Zn ferrite nanoparticles for ferrofluid preparation: Study on magnetic properties. *Physica B: Condensed Matter*, *363*(1-4), pp.225-231.

[13] Price, S.D. and Roithová, J., 2011. Multiply charged ions in the gas phase. *Physical Chemistry Chemical Physics*, *13*(41), pp.18251-18252.

[14] Thakur, A., Verma, R., Wan, F., Ravelo, B., Edelman, I., Ovchinnikov, S. and Thakur, P., 2023. Investigation of structural, elastic and magnetic properties of Cu^{2+} ions substituted cobalt nano ferrites. *Journal of Magnetism and Magnetic Materials*, *581*, p.170980.

[15]Rani, B.J., Ravi, G., Yuvakkumar, R., Ganesh, V., Ravichandran, S., Thambidurai, M., Rajalakshmi, A.P. and Sakunthala, A., 2018. Pure and cobalt-substituted zinc-ferrite magnetic ceramics for supercapacitor applications. *Applied Physics A*, *124*, pp.1-12.

[16]Coppola, P., Da Silva, F.G., Gomide, G., Paula, F.L.O., Campos, A.F.C., Perzynski, R., Kern, C., Depeyrot, J. and Aquino, R., 2016. Hydrothermal synthesis of mixed zinc–cobalt ferrite nanoparticles: structural and magnetic properties. *Journal of Nanoparticle Research*, *18*, pp.1-15.

[17]Chahar, D., Taneja, S., Bisht, S., Kesarwani, S., Thakur, P., Thakur, A. and Sharma, P.B., 2021. Photocatalytic activity of cobalt substituted zinc ferrite for the degradation of methylene blue dye under visible light irradiation. *Journal of Alloys and Compounds*, *851*, p.156878.

[18]Shakil, M., Inayat, U., Khalid, N.R., Tanveer, M., Gillani, S.S.A., Tariq, N.H., Shah, A., Mahmood, A. and Dahshan, A., 2022. Enhanced structural, optical, and photocatalytic activities of Cd–Co doped Zn ferrites for degrading methyl orange dye under irradiation by visible light. *Journal of Physics and Chemistry of Solids*, *161*, p.110419.

[19]Ibrahim, I., Ali, I.O., Salama, T.M., Bahgat, A.A. and Mohamed, M.M., 2016. Synthesis of magnetically recyclable spinel ferrite (MFe2O4, M= Zn, Co, Mn) nanocrystals engineered by sol gel-hydrothermal technology: High catalytic performances for nitroarenes reduction. *Applied Catalysis B: Environmental*, *181*, pp.389-402.

[20]Ortiz-Quiñonez, J.L., Pal, U. and Villanueva, M.S., 2018. Structural, magnetic, and catalytic evaluation of spinel Co, Ni, and Co–Ni ferrite nanoparticles fabricated by low-temperature solution combustion process. *ACS Omega*, *3*(11), pp.14986-15001.

[21]Sajjad, M., Ali, K., Jamil, Y., Sehar, S., Akbar, L., Tahir, M. and Alzaid, M., 2021. Effect of Zn substitution on the structural, magnetic, optical, and electrical properties of low-temperature-synthesized cobalt ferrites. *Journal of Materials Science: Materials in Electronics*, *32*, pp.6001-6013.

[22]Phong, P.T., Nam, P.H., Phuc, N.X., Huy, B.T., Lu, L.T., Manh, D.H. and Lee, I.J., 2019. Effect of zinc concentration on the structural, optical, and magnetic properties of mixed Co-Zn ferrites nanoparticles synthesized by low-temperature hydrothermal method. *Metallurgical and Materials Transactions A*, *50*, pp.1571-1581.

